

The Effect of River Water Circulation on the Distribution and Functioning of Reservoir Microbial Communities as Determined by a Relative Distance Approach

Karel Šimek,^{1,2*} Marta Comerma,³ Juan-Carlos García,^{3,4} Jiří Nedoma,¹ Rafael Marcé,^{3,5} and Joan Armengol³

¹Biology Centre of the Academy of Sciences of the Czech Republic, v.v.i., Hydrobiological Institute, Na Sádkách 7, 37005 České Budějovice, Czech Republic; ²Faculty of Science, University of South Bohemia, Na Sádkách 7, 37005 České Budějovice, Czech Republic; ³Department of Ecology, Fluvial Dynamics and Hydrological Engineering (FLUMEN), University of Barcelona, Diagonal, 645, 08028 Barcelona, Spain; ⁴Aigües Ter-Llobregat (ATLL), c/Afores, s/n, Caddeu, 08044 Barcelona, Spain; ⁵Catalan Institute for Water Research (ICRA), Scientific and Technological Park of the University of Girona, H₂O Building, Emili Grahit 101, 17003 Girona, Spain

ABSTRACT

The effect of river water quality, its inflow rate, and temperature on planktonic food web composition and activities were studied in the eutrophic Sau Reservoir (Catalonia, NE Spain). We analyzed 8 longitudinal transects conducted between July 1996 and April 1999 covering a wide range of variability in both seasonal and spatial circulation patterns. To compare objectively the biological longitudinal gradients under seasonally fluctuating water levels and different types of water circulation

patterns, we applied a model based on the relative distance of a sampling station from the river inflow. Even under different hydrological scenarios, the model was able to characterize epilimnetic food chain successions and locations of peaks of bacteria, heterotrophic nanoflagellates, ciliates, phytoplankton, and zooplankton along the longitudinal gradient. The amplitude of microbial peaks was directly related to the proportion of nutrient and organic carbon rich river water that mixed into the reservoir epilimnion. Enhanced abundances and activities of microbes were detected in spring and summer periods, mainly during events of river water overflow when a large proportion of the river was directly mixed into the epilimnion. Thus, the relative input of river water is suggested to be a useful predictor of the amplitude of the development of the epilimnetic microbial food webs in highly loaded canyon-shaped reservoirs. These results may have important implications in the context of global change in Mediterranean regions,

Received 26 April 2010; accepted 27 August 2010;
published online 7 October 2010

Author Contributions: KS participated in sampling, suggested statistical evaluation of the data allowing to distinguish the effect of different water circulation patterns and wrote the paper. MC organized the sampling program and suggested the relative distance model as a tool to evaluate the data from different seasons. JCG organized field work and participated in the sampling program. JN ran the statistics and suggested the standardization of the relative distance model. RM contributed with discussions and improved the text and presentation. JA suggested the sampling strategy and coordinated the research program.

*Corresponding author; e-mail: ksimek@hbu.cas.cz

where expected reductions in runoff may profoundly affect river water circulation patterns in reservoirs and hence organic carbon cycling in these ecosystems.

INTRODUCTION

Man-made reservoirs are important sites for carbon processing at local (Weissenberger and others 2010) and global scales (Seitzinger and others 2005). Herein, microbial communities play a fundamental role in organic matter processing, especially in reservoirs receiving large amounts of organic matter (Uhlmann 1991). However, drivers governing bacterial activity in flushed systems like reservoirs are still poorly understood, mainly because there are too few data to describe the major microbial processes which significantly affect organic carbon processing and oxygen saturation in reservoir ecosystems. Although dam reservoirs are considered as “lake-like” man-made water bodies, in reality they differ from natural lakes substantially (Straškraba 1998). The most pronounced differences are found with regard to typical canyon-shaped reservoirs because they are spatially highly heterogeneous systems with relatively short water retention times and typically exhibit pronounced spatial gradients from the river inflow to their dam area (Thornton and others 1990; Straškraba and others 1993). Nutrient and organic matter loads in riverine input, morphology and hydraulic retention time have been frequently suggested as major factors affecting downstream reservoir plankton succession, rates of biological processes, and resulting water quality in reservoirs (Straškrabová 1976; Šimek and others 1998; Gasol and others 2002; Comerma and others 2003). However, the interplay of these factors with river hydrodynamics has not been studied yet.

Three types of river water circulation patterns can be distinguished in temperate canyon-shaped reservoirs (Kennedy and Walker 1990; Armengol and others 1999): (i) underflow when the inflow water temperature is colder than that of the whole water column in the reservoir and thus the river water flows at the bottom; (ii) interflow when the inflow water is colder than that of the reservoir surface layers but warmer than in the bottom reservoir layer; and (iii) overflow when the inflow river water and the epilimnetic reservoir water masses have similar temperatures. Although effects of changing hydrodynamics on major physical and chemical parameters in canyon-shaped reservoirs

Key words: canyon-shaped reservoir; river–reservoir ecosystem; longitudinal gradients; water circulation patterns; plankton succession; microbial dynamics; relative distance model.

have been studied over the last two decades (for example, Thornton and others 1990; Straškraba 1998; Armengol and others 1999), their effects on the spatial and temporal variability of biological variables have been investigated only recently (for example, Comerma and others 2001; Šimek and others 2001; Mašín and others 2003). The biological gradients are initiated by the activity of microbial food webs owing to the small cell size, high uptake capabilities, and growth rates of planktonic microorganisms. In eutrophic reservoirs, typical downstream succession of heterotrophic microbial communities from the river inflow (for example, bacteria–flagellates–ciliates) has been observed (Šimek and others 2001; Comerma and others 2003; Jezbera and others 2003). The longitudinal position and amplitude of the abundance peaks of microbial food web members vary temporally. It has been hypothesized that water circulation patterns in the reservoir play a key role in these processes (Comerma and others 2003), because even the same quality and quantity of the inflow river water may have markedly different impacts on downstream epilimnetic plankton succession, depending on the water circulation pattern within a reservoir. However, a convincing demonstration of this hypothesis has proven to be elusive, because river water temperature, flow rate, and quality of resources limiting the growth rates of plankton communities vary greatly with the seasons. Moreover, reservoirs tend to exhibit large seasonal fluctuations in water level, yielding dramatic changes in the length of an impoundment, which limits comparability of longitudinal and seasonal succession trends.

To examine the spatio-temporal changes in plankton dynamics, we chose a specific model system, the Sau Reservoir (NE Spain), affected by the Mediterranean climate. The system displays large seasonal fluctuations in water levels and temperature (Armengol and others 1999), which have significant socio-economic impacts because the reservoir forms the upper part of a cascade of two reservoirs designated as drinking facilities for the city of Barcelona. The Sau Reservoir has been characterized as showing: (I) high nutrient and organic matter inputs (Šimek and others 2001;

Comerma and others 2003; Marcé and others 2004); (II) morphology typical for a deep and narrow river valley reservoir (Armengol and others 1999); and (III) a typical water residence time of about 90 days. Thus, we anticipated finding clear longitudinal patterns and relationships between limnological and biological parameters along the reservoir even over different seasons of a year. We hypothesized that development and the maxima of bacterial, HNF and ciliate communities, and thus organic carbon processing (Comerma and others 2003, Marcé and others 2006), are directly related to the proportion of nutrients and organic matter rich river water that is mixed into the reservoir epilimnion.

To test these hypotheses, we analyzed 8 sampling campaigns conducted between 1996 and 1999 covering all seasonal aspects of the hydrology of the reservoir. Then we examined their spatial heterogeneity using a relative distance model that allows standardization of the typical patterns in plankton succession under different hydrological situations. Study aims were: (i) to propose a general method that allows for the comparison and prediction of common trends in the spatial dynamics of plankton communities and their functioning under different hydrological scenarios in canyon-shaped reservoirs; and (ii) to specifically analyze the influence of overflow events on organic carbon processing and oxygen saturation levels of the epilimnetic layer of the Sau Reservoir.

MATERIALS AND METHODS

Study Site and Sampling

The Sau Reservoir is a 18.5 km long, canyon-type eutrophic reservoir located in the middle stretch of the river Ter (Catalonia, NE Spain, 41°58'N, 2°25'E, 426 m a.s.l., max. area 7.6 km², max. volume 167 × 10⁶ m³, max. depth 75 m, mean depth 25 m, mean hydraulic retention time 90 days, mean inflow river rate of 12.8 m³ s⁻¹, monomictic). For a detailed description of the reservoir, see Armengol and others (1999) and Comerma and others (2001). We collected samples at nine fixed stations equidistantly located at approximately 1.8 km intervals along the main axis of the reservoir from the river inflow downstream (Figure 1). We conducted 8 sampling campaigns in different seasons (see Table 1). Depending on current water level and the corresponding length of the reservoir, the number of sampled stations varied from 8 to 9, except for the Apr-99 sampling when due to extreme drought only 4 reservoir stations were available. Note that the sampling set covers a wide range of hydrological situations (Table 1), which is not at odds with the marked Mediterranean climate in the region. The range of observed volumes embraces nearly 70% of the values in the historical distribution of daily volume records in the reservoir during the last 30 years (median = 109 × 10⁶ m³, 2.5% and 97.5% quantiles = [35, 147]). Comparatively, the observed range of inflow values was

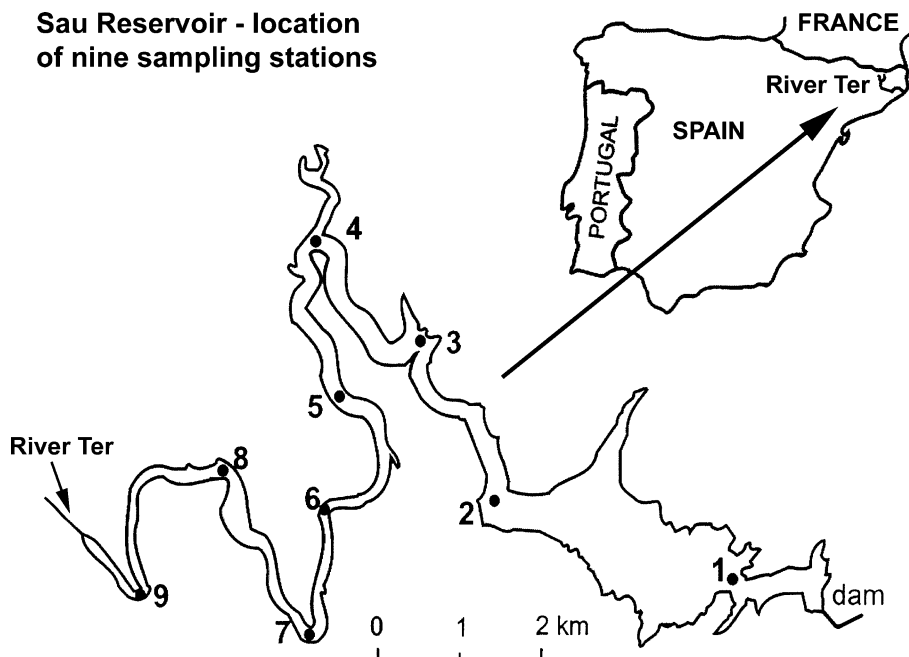


Figure 1. Scheme of the Sau Reservoir, situated in North East Spain, with nine sampling stations located approximately equidistantly from the Ter river inflow towards the dam of the reservoir.

Table 1. Major Hydrological Descriptors of the Sau Reservoir for Each Longitudinal Transect

Date	Current inflow ($\text{m}^3 \text{ s}^{-1}$)	Previous inflow (15 days) ($\text{m}^3 \text{ s}^{-1}$)	Reservoir volume (10^6 m^3)	Outflow ($\text{m}^3 \text{ s}^{-1}$)	Plunge point km from the river	$T_{\text{epil}} - T_{\text{river}}$ ($^{\circ}\text{C}$)	River water mixed % (Cond.)	Circulation pattern
Jul-96	9.9	10.1	113	24.0	4.3	3.8	24	Interflow
Apr-97	11.6	12.7	114	5.6	4.5	1.8	75	Overflow
Jul-97	13.2	24.9	122	23.3	6.9	2.5	14	Interflow
Oct-97	4.1	4.0	118	8.8	4.8	4.5	36	Interflow
Dec-97	13.1	6.2	129	23.5	4.3	5.2	15	Underflow
Feb-98	5.7	9.3	103	2.5	7.6	0.8	51	Overflow
May-98	7.3	9.2	116	1.3	6.4	1.0	88	Overflow
Apr-99	4.8	5.3	44	4.7	11.5	0.8	–	Overflow

Current inflow rate is the mean value over two days when the longitudinal transect was sampled.

Previous inflow represents the mean value of the river inflow rate over a period of 15 days prior to starting the longitudinal sampling of the reservoir.

T_{epil} and T_{river} are temperatures of the reservoir epilimnion and river inflow, respectively.

% (Cond.)—conductivity based estimate of percentage of river water mixed in the epilimnion.

The above descriptors were used to detect the plunge point position, type of water circulation pattern and proportion of river water admixed to the epilimnion of the Sau reservoir in 8 longitudinal transects: July 1996, April 1997, July 1997, October 1997, December 1997, February 1998, May 1998, and April 1999.

narrower (Table 1), only embracing 40% of the values in the 30-year historical daily record (median = $8.05 \text{ m}^3 \text{ s}^{-1}$, 2.5% and 97.5% quantiles = [1.3, 61.5]). However, this was a direct consequence of the sampling strategy, because we consciously avoided sampling just after flooding periods to study the biological communities and their succession close to their possible steady-state.

At each sampling station we measured 1 m resolution vertical profiles of temperature, pH, oxygen concentration, conductivity, and nephelometric turbidity from the surface to the bottom, using a YSI-Grant Water Quality Logging System (model 3600) multiprobe. Integrated water samples from the epilimnion were collected for chemical and biological analyses with a plankton tube sampler (3–5 m long) and samples were stored in 5 l, dark, plastic bottles prior to analyses. The temperature, dissolved oxygen, and conductivity profile data were measured with the YSI-Grant probe to (i) detect the epilimnetic layer (Z_{mix}) and then (ii) to collect representative samples of the epilimnetic mixing layer from the surface to the depth of Z_{mix} . The mixing layer in the Sau Reservoir very seldom goes below a 5 m depth. Obviously, this sampling scheme implies that, as we move downstream, a smaller proportion of water column is accounted for. However, in the vast majority of cases, the upper 5 m represented the whole epilimnion, which was the target part of the water column for our study. Samples were collected within 2–3 days, starting from the river downstream. We have estimated that the movement of the river water mass should have no effect on the samples collected downstream within the 2–3 days sampling period.

Hydrological Descriptors

Current inflow rate, volume of the reservoir and outflow were calculated from the averages of the sampling days and the days prior to sampling (Table 1), provided by the Catalan Water Agency. The inflow volume preceding sampling was estimated from the average of inflows for 15 days before sampling began. The location of the plunge point (that is, the border between the riverine and the lacustrine zones of the reservoir) was calculated using the model developed by Imberger and others (1978) as detailed in Armengol and others (1999):

$$L_0 = h_0 / \tan \alpha \quad (1)$$

where L_0 is the location of the plunge point expressed as the distance from the river gauge, α is the slope of the streambed, and h_0 is the water column depth at the plunge point, a complex function including streamflow, density gradients, and streambed morphology. After locating the plunge point, we estimated the initial mixing of river water with reservoir water downstream of the plunge point using mass balances of conservative natural tracers as specified by Armengol and others (1999). We calculated a simple dilution model:

$$\begin{aligned} C_R a + C_E b &= C_P(a + b) \\ (a + b) &= 100 \end{aligned} \quad (2)$$

where C_R is conductivity in the river, C_E in the epilimnion of the reservoir, and C_P just after the plunge point. a and b are adjustable parameters, a standing for the proportion of river water mixed in the epilimnion.

The insertion depth of the reservoir (that is, the depth at which the river water enters in the reservoir after the plunge point) was calculated assuming that water density is mainly determined by temperature. Basically, when the river water is warmer than the reservoir water the river flows as an overflow; when the river is colder than the deep waters of the reservoir the river flows as an underflow; and interflows happen in the rest of intermediate situations (see Figure 2A). The suitability of this method has been repeatedly confirmed by previous work in this reservoir using multiparametric profiles along the reservoir (Armengol and others 1999; Marcé and others 2008) and modeling exercises (Vidal 2007).

Chemical Analysis

Water samples for determination of concentrations of chloride, dissolved organic carbon (DOC), biodegradable dissolved organic carbon (BDOC) and dissolved reactive phosphorus were filtered through GF/F pre-combusted Whatman filters (GF-5 with nominal porosity of 0.4 μm , Macherey–Nagel, Düren, Germany, temperature 450°C for 4 h). Chloride concentration (mg l^{-1}) was measured in 1 ml of filtered water in a Konik (model KNK 500-A) liquid chromatograph.

DOC was analyzed in filtered samples with a TOC 5000A analyzer (Shimadzu, Japan). The amount of BDOC was determined by a modified method of Servais and others (1987). Briefly, 200 ml of filtered sample (GF-5 filters) was added to duplicate 250 ml glass bottles, along with 1 ml of the original water sample, which was filtered through polycarbonate filters with porosity of 0.8 μm (OSMONIC INC., Livermore, USA) to remove bacterivores. The water was then incubated in the dark at 20°C for 28 days. After this incubation, the absence of protistan bacterivores was checked microscopically and the sample was again filtered through GF-5 filters to determine DOC concentrations. BDOC was calculated as the difference between DOC concentrations before and after the incubation. A blank determination was carried out by the same procedure but using deionized water instead of sample.

Total phosphorus (TP) was measured directly in the non-filtered water according to the method of Grasshoff and others (1983). Dissolved reactive phosphorus (DRP as $\text{PO}_4\text{-P}$) was analyzed according to Murphy and Riley (1962) using a Shimadzu spectrophotometer (UV-1201) at 890 nm. Total nitrogen was determined in non-filtered water according to Grasshoff and others (1983). Briefly,

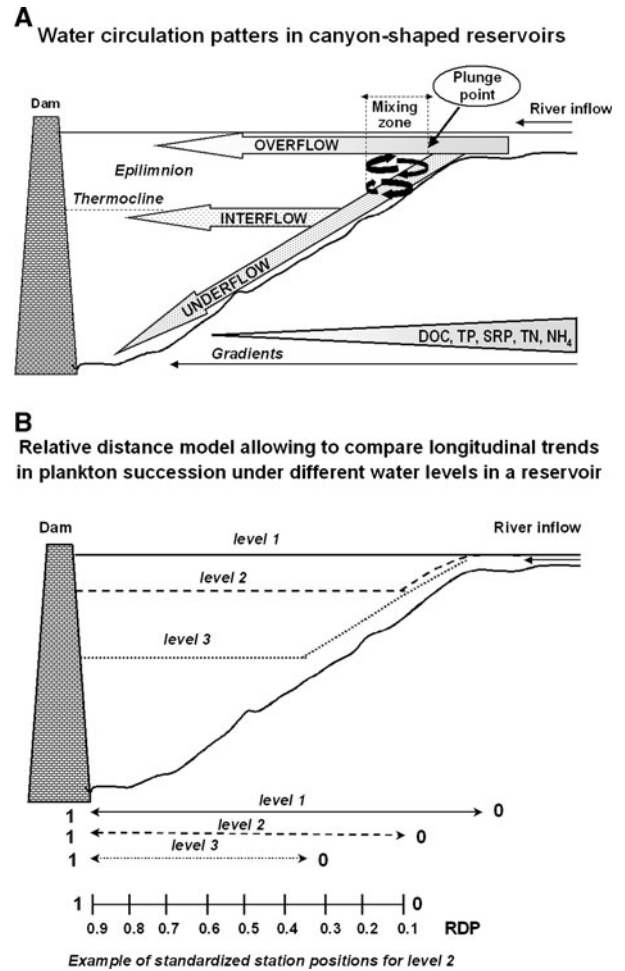


Figure 2. **A** Schematic drawing of water circulation patterns, that is, over-, inter-, and underflow, in deep canyon-shaped reservoirs. Depending on water temperature and water quality parameters river water masses plunge to different strata of the reservoir. From the plunge point downstream a transient mixing zone starts with a very strong gradient in water quality parameters (for details see the text). In addition to the type of water circulation pattern, chemical and biological downstream longitudinal gradients are directly related to the differences between the river and reservoir water quality parameters, mainly in organic carbon and nutrient availability. *DOC* dissolved organic carbon, *TP* total phosphorus, *SRP* soluble reactive phosphorus, *TN* total nitrogen, *NH₄* ammonium. **B** Schematic drawing of the effect of different water levels (level 1–3) on the total length of the reservoir. To facilitate a comparison of common features of longitudinal gradients under fluctuating water levels, a relative distance model is exploited, where the actual length of the reservoir is always subdivided into the same number of standardized nine sampling positions (“alignment positions”) rounded to one decimal place between zero and one (for details see the text). An example of standardized relative distance positions (RDP) is given for the level 2 that corresponds to a medium decreased water level of the reservoir.

the samples were digested with an oxidizing reagent inside of Teflon tubes (110°C, 90 min) to transform total nitrogen to nitrate, which was determined by colorimetry. Ammonium concentrations were measured according to Solorzano (1969) using a Technicon AutoAnalyzer at 630 nm.

Bacterial Abundance, Biomass, and Production

Subsamples were fixed with formaldehyde (2% final concentration), stained with DAPI (4',6-diamidino-2-phenylindole, 0.2% wt/vol), filtered on 0.2 µm black filters (OSMONIC INC., Livermore, USA), and enumerated via epifluorescence microscopy (OLYMPUS, AX-70). Semiautomatic image analysis (Lucia, Laboratory Imaging, Prague) was used for sizing more than 400 bacteria per sample (for details see Šimek and others 2001).

Bacterial production was measured at in situ temperature following the method described by Bell (1993), using the protocol of [*methyl*-³H] thymidine incorporation into total macromolecules (cold TCA insoluble fraction, for details see Comerma and others 2001). By using a grazer-free (pre-filtered through 1 µm-pore-size filters) mixed bacterial population from the reservoir in a batch culture, we established an empirical conversion factor (ECF) between cell production rate and thymidine incorporation for each sampling campaign. The mean from all empirical ECFs (4.7×10^{18} cells mol⁻¹ thymidine incorporated, SE = 0.98×10^{18} cells, $n = 13$) was used to estimate bacterial production.

Chlorophyll *a*

Chlorophyll *a* (Chl-*a*) content in phytoplankton collected on GF/F Whatman filters was analyzed by using a trichromatic method (Jeffrey and Humphrey 1975).

Protozoan Abundance and Grazing

Protozoan bacterivory was estimated using fluorescently labeled bacteria (FLB) concentrated from the reservoir water. We took a 300-ml subsample of an integrated water sample from the epilimnion that was incubated in Pyrex bottles with an FLB addition accounting for 5–20% of natural bacterial abundances. Heterotrophic nanoflagellate (HNF) and ciliate abundances and FLB uptake rates were determined in short-term FLB direct-uptake experiments described in detail in Šimek and others (1995, 2001).

Zooplankton

Vertical hauls over 20 m were done using a 53-µm mesh Apstein net, thus yielding depth-integrated zooplankton samples from the upper 20 m. This minimized the possible effect of zooplankton migration during daylight periods to the deeper reservoir strata (Seda and others 2007). When the water column depth was less than 20 m we collected zooplankton from the bottom to the surface. Zooplankton samples were preserved in 4% formaldehyde (final concentration). Subsamples were placed in a sedimentation chamber and Cladocera, copepods, nauplii and rotifers were quantified in an inverted microscope (Olympus T041, for details see the method of McCauley 1984).

Modeling Longitudinal Plankton Patterns

To standardize data for the calculation of longitudinal patterns, both station positions and the measured variables were normalized. To normalize nine station positions (compare Figure 1), first, for each transect, the relative station positions along the reservoir were expressed as the ratio of the distance of a station from the actual river inflow and of the current total reservoir length taken from inflow (relative position equal to 0) to dam (relative position equal to 1, see Figure 2B). Then, to allow matching and averaging of data from different transects, the relative station positions were rounded up or down to one decimal place, thus obtaining 9 corrected relative station positions (or “alignment positions”), that is, 0.1, 0.2, and so on up to 0.9. These are referred to as relative distance positions (RDP) throughout the text and in the figures. The values 0 and 1.0 did not occur in any of the transects. To normalize measured data values (to standardize the statistical weight of the data originating from different transects), first, for each transect, the average value of each variable was calculated and the data from individual stations expressed as percentages of this transect average. Then, the percentage data from different transects from matching RDPs were averaged. Finally, to ensure comparability between different variables, for each variable of bacteria, HNF, ciliates, phyto-, and zooplankton (Figure 3) the obtained percentages were corrected to give a sum of 100% over the transect (that is, over 9 RDPs from 0.1 to 0.9) and plotted against these RDPs. This data treatment facilitates examining common features of plankton succession under conditions of different water levels, lengths of the reservoir, and water circulation patterns.

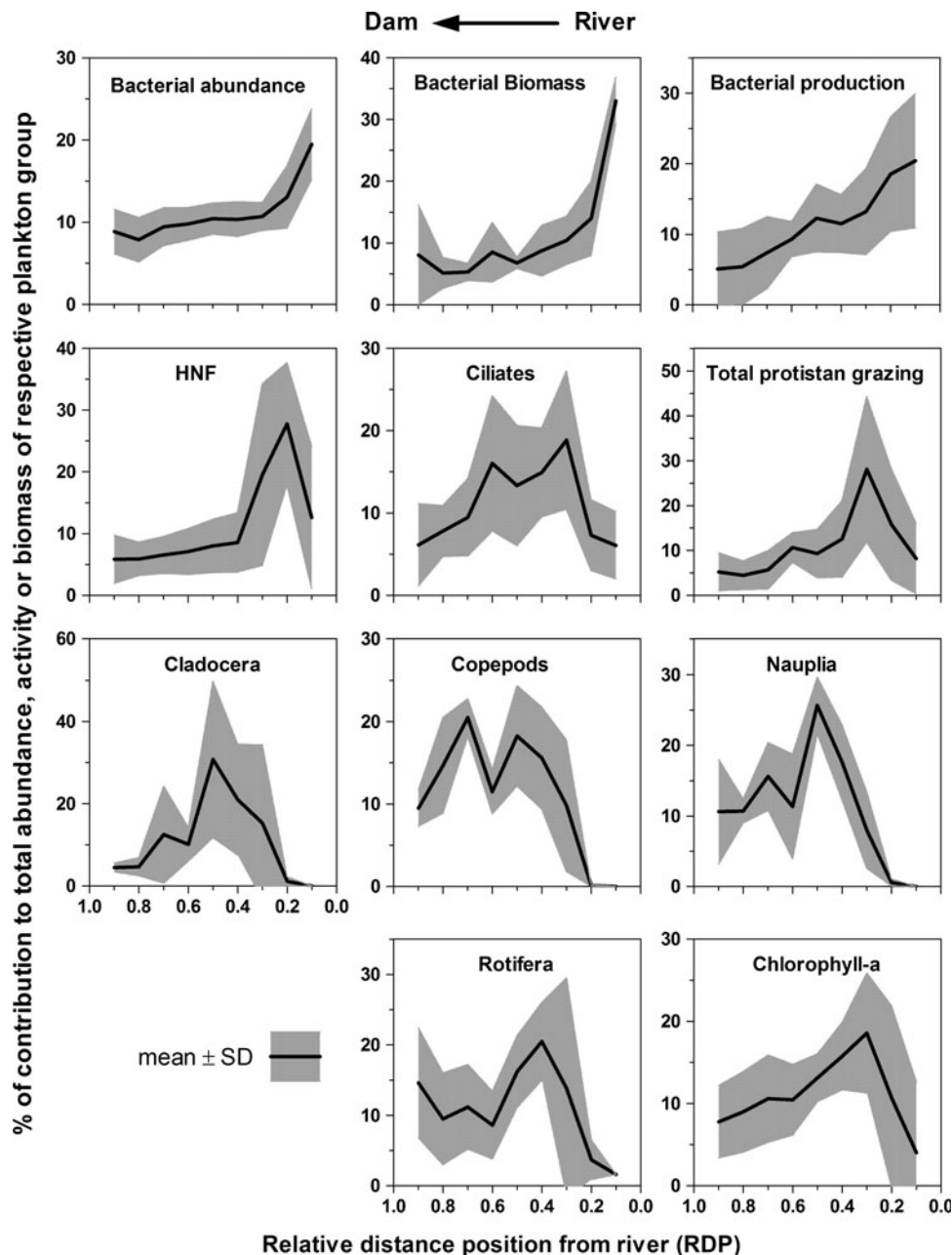


Figure 3. Standardized characteristic downstream succession of plankton communities based on the relative distance model and rounded relative distance positions (RDP) of percentage of bacterial, HNF, ciliate and zooplankton abundances, bacterial biomass and production, total protozoan bacterivory, and chlorophyll *a* concentrations evaluated in 8 longitudinal transects (see Table 1 for details). Note that percentage values plotted against 9 RDPs, that is, 0.1, 0.2, ... 0.9, gives a sum of 100% over the longitudinal transect. The values are means and the *gray filled area* shows $\pm 1SD$.

RESULTS

Major Features of Downstream Gradients in the Reservoir

We found strong gradients in basic chemical and bacterioplankton abundance data, yielding a decreasing trophic status from the river inflow towards the lacustrine part of the Sau Reservoir (Table 2). Although station 5 represents an intermediate location, lacustrine station 1 always significantly differed from the river inflow in the studied parameters. The bulk DOC also decreased significantly downstream, but its biodegradable

proportion (BDOC) decreased even more so along the same longitudinal gradient, that is, by a factors of about 4 and 3 at stations 1 and 5, respectively (Table 2).

Standardized Longitudinal Succession of Epilimnetic Communities

In Jul-96, Apr-97, Jul-97, Oct-97, and Dec-97 the water level allowed us to sample all 9 sampling stations (compare Figure 1), but due to a lower water level in Feb-98 and May-98, only stations 1–8 could be sampled, and only stations 1–4 were

Table 2. Basic Chemical and Bacterioplankton Abundance Data at Three Stations Along the Longitudinal Profile of the Sau Reservoir

Parameter	Significance	Station 1 (lacustrine)	Station 5 (middle)	Station 8 or 9 (river inflow)
DRP ($\mu\text{g l}^{-1}$)	$P < 0.002$	12 (1–24) ^A	21 (5–37) ^A	68 (35–135) ^B
TP ($\mu\text{g l}^{-1}$)	$P < 0.007$	74 (28–112) ^A	106 (84–137) ^{AB}	185 (141–269) ^B
TN (mg l^{-1})	$P < 0.04$	2.8 (1.5–2.9) ^A	3.0 (2.2–4.0) ^{AB}	6.2 (4.2–11.1) ^B
NH ₄ -N (mg l^{-1})	$P < 0.03$	0.5 (0.3–0.7) ^A	1.3 (2.2–4.0) ^{AB}	4.6 (2.6–6.3) ^B
DOC (mg l^{-1})	$P < 0.02$	2.8 (2.5–3.2) ^{AB}	2.8 (2.2–3.1) ^A	4.3 (3.1–5.3) ^B
BDOC (% of DOC)	$P < 0.005$	11 (8–17) ^A	16 (12–24) ^{AB}	45 (28–60) ^B
Bacteria (10^6 ml^{-1})	$P < 0.001$	4.17 (1.64–5.90) ^A	5.41 (2.54–8.59) ^A	9.8 (4.32–16.1) ^B

Station 1 is close to the reservoir dam, station 5 is situated in the middle of the reservoir, and stations 8 or 9 represent most frequently the position of the Ter river inflow (see Figure 1 for location of the stations).

Values are means of 8 (station 1 and 5) or 7 sampling campaigns (station river inflow) with range of values given in parenthesis. Values in the same row labeled with different superscript letters (^A or ^B) are significantly different from each other ($P < 0.05$, Kruskal–Wallis test followed by Dunn's Multiple Comparison Test).

DRP dissolved reactive phosphorus, TP total phosphorus, TN total nitrogen, NH₄-N ammonium nitrogen, DOC dissolved organic carbon, BDOC biodegradable organic carbon.

sampled in Apr-99 due to the extremely low water level. Thus, except for Apr-99, stations 9 and 8 (Figure 1) represented typically riverine stations, stations 7 and 6 transient stations with the plunge point situated from station 8 downstream to station 6 (Table 1), and stations 5 to 1 represented mostly lacustrine parts of the reservoir. Down- and upstream shifts in the longitudinal dynamics over time were related to reservoir length or the flow rate of the inflow river affecting the position of the plunge point (Table 1).

All longitudinal transects had common features of mean abundance or concentrations, highlighting the value of the standardized station position approach (see Figure 3). These plots of microbial, phyto-, and zooplankton data revealed the following trends. Due to high nutrient and BDOC input (Table 2), bacterial abundance, biomass and production clearly peaked in the riverine part of the reservoir. This river-born, huge bacterial biomass was followed by a peak of HNF abundance at relative distance position (RDP) 0.2 from the river, yet within the transient reservoir part. Two peaks of ciliates were usually composed of different groups: the first peak, near the inflow (0.3 RDP), consisted of bacterivorous ciliates and the second one, in the middle of the reservoir (0.6 RDP), was mainly composed of algivorous ciliates (M. Comerma, unpublished data). As a consequence of the spatial overlap between high HNF abundance and bacterivorous ciliate peak abundance, a marked peak in total protozoan bacterivory was situated at the lower part of the transient reservoir zone (0.3 DRP) where Chl-*a* concentrations peaked. Large zooplankters, that is, cladocerans and copepods, were absent in the river inflow and only rotifers

appeared there in low numbers. All zooplankton groups, except rotifers, showed bimodal distributions that were substantially shifted downstream with the rotifer first peak shifted slightly upstream (0.4 RDP, just after the Chl-*a* maximum). In contrast, the abundances of cladocerans, copepods, and nauplii were highest in the middle of the reservoir (at 0.5 RDP) where Chl-*a* concentrations were gradually decreasing. All zooplankton groups commonly developed a second, less marked abundance peak in the lower, lacustrine part of the reservoir (0.7 RDP). Regardless of the high availability of nutrients in the river inflow (Table 2), Chl-*a* reached maximum values further downstream, at the transient zone of the reservoir (Figure 3), where increased water transparency allowed enhanced phytoplankton growth.

Impacts of Water Circulation Patterns on Spatial Food Web Succession

Hydrological conditions (Table 1) determined the type of river water circulation that in turn affected nutrient and organic carbon loadings from the River Ter to the epilimnion of the reservoir. These nutrients, apparently mainly the high proportion of BDOC in DOC (on average 45%, Table 2), also initiated strong gradients downstream of the river.

Using the hydrological features (Table 1), the sampling campaigns were divided into overflow (Apr-97, Feb-98, May-98, and Apr-99), interflow (Jul-96, Jul-97, and Oct-97), and underflow (Dec-97) circulation patterns. For instance, when the river temperature was notably lower than in the epilimnion (Jul-96, Jul-97, Oct-97, and Dec-97), the river water masses plunged to the hypolimnion

near the river inflow, with only 14–36% of river water injected into the epilimnion. Notably, the proportion of river water that mixed with the epilimnion in cases when the river circulated below the epilimnion, depended also on the river flow rate. We usually found a lower portion of river water injected into the epilimnion when the river flow was high, except for Apr-97 (see Table 1). For other dates, with moderate to low river flow rates and similar temperatures of the river and epilimnion, the proportion of river water mixing with the epilimnion was very high (51–88%).

Maximum bacterial, HNF and ciliate abundances occurred in Apr-97 (for details see Šimek and others 2001), Feb-98, and May-98, when proportions of river water mixing with the epilimnion were very high (Table 1). However, the most significant effects of the river-borne nutrients were obvious for heterotrophic bacterioplankton. Maximum bacterial abundance, cell volume, and production were tightly correlated with the percentages of the BDOC-rich river water mixed with the epilimnion over all sampling campaigns ($r^2 = 0.585$, $r^2 = 0.674$, $r^2 = 0.770$, respectively; $P < 0.05$, $N = 8$). Consequently, the abundance of typical protistan bacterivores, HNF and ciliates, mostly tightly reflected the percentage of river water mixed with the epilimnion. A significant downstream drop of the proportion of BDOC in DOC obviously supported the enhanced microbial dynamics (compare Table 2 and Figure 4). Note that these results are at odds with the fact that water temperature was higher during interflows and underflows (Figure 4), which should even promote bacterial activity.

To test more quantitatively the effect of water circulation on the downstream succession of various microbial groups, we used the relative distance model and plotted the means of selected microbial variables for overflow versus pooled inter- and underflow events for each RDP (Figure 4). This analysis clearly indicated significantly higher abundance and production of heterotrophic bacterioplankton in the inflow and middle parts of the reservoir during overflow situations. Remarkable peaks of HNF and ciliate abundance developed at RDP 0.3 (usually around or just after the plunge point). Their total rates of bacterivory during overflow events were significantly higher than during the inter- and underflow events. Interestingly, the downstream growth stimulation of ciliates was apparently bimodal and more pronounced towards the middle of the reservoir than that of HNF (Figure 4). Chl-*a* showed an opposite trend to

other parameters, with lower concentrations in inflow parts during the overflow compared to pooled inter- and underflow events (Figure 4). However, in the downstream reservoir parts Chl-*a* concentrations were already consistently higher during the overflow events. The enhanced microbial abundances and activities during the overflow events were also reflected in significantly lower oxygen saturation in the riverine section (Figure 4, RDP of 0.1–0.6) with prevalence of sub-saturating conditions. Thus interestingly, the degradation of BDOC in the inflow reservoir parts resulted in disconnecting oxygen super saturation (RDP 0.5–0.9) from the maxima of Chl-*a* (RDP 0.2 and 0.4, see Figure 4). Moreover, the enhanced influx of labile organic carbon in the inflow river (Table 2) overrode the effect of higher temperatures on microbial variables during the inter- and underflow events and notably the sub-saturating oxygen concentrations appeared more frequently under generally lower temperatures during the overflow events (Figure 4).

Typical successions of bacteria, HNF, and ciliates (Figures 3, 4) indicated that the strongest influence of water circulation patterns (Figure 2A) on the epilimnetic communities was within 5–6 km downstream from the plunge point where the effect of the BDOC-rich river should be strongest. Thus, data from four stations below the plunge point (situated within ~5.5 km) were averaged separately to compare overflow versus inter- and underflow events (Figure 5). This data treatment showed a consistent trend of higher microbial variables for the river overflow compared to the inter- and underflow events. These differences were significant for all variables (*t* test, $P \leq 0.04$), except HNF abundance ($P = 0.057$) which varied more than the other microbial variables (Figures 4, 5).

DISCUSSION

Effect of Water Circulation Pattern on Plankton Succession

Building on a robust dataset, we detected significant relationships between the amount of BDOC-rich river water (Table 1) mixed into the reservoir epilimnion and amplitudes of the development and activity of major components of microbial plankton food webs. By combining the relative distance model with the model describing water circulation patterns (Armengol and others 1999) our study provides novel insights into major factors affecting the longitudinal dynamics of the

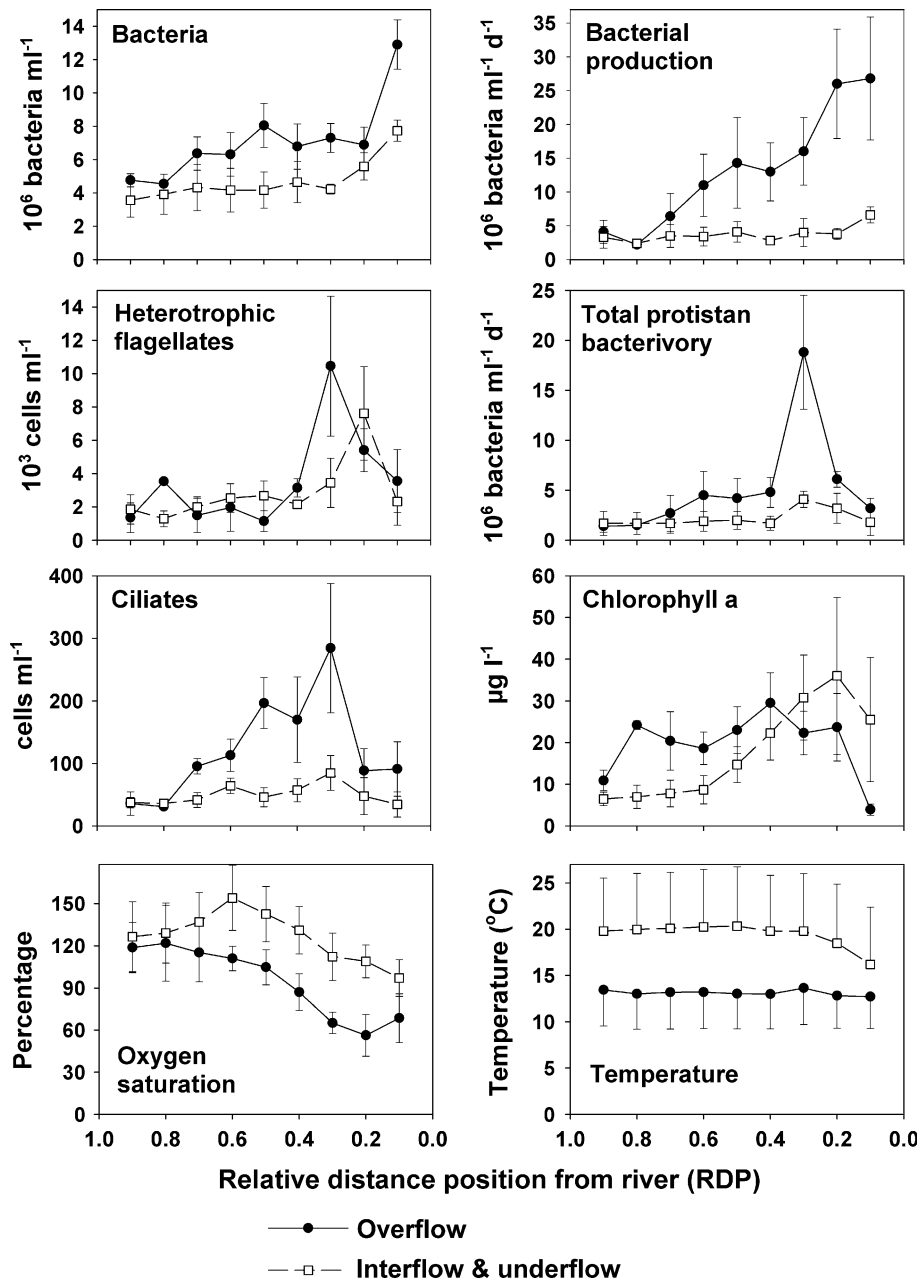


Figure 4. Using the relative distance model the average values of microbial abundance and activity parameters and oxygen saturation are plotted separately for overflow (4 samplings, for details see Table 1) versus pooled inter- and underflow events (4 samplings) for each standardized station (RDP) on the longitudinal gradient through the Sau Reservoir (compare Figure 2B). Oxygen saturation and temperature data represent mean epilimnetic values for the upper 4 m (that is, 0, 1, 2, 3, and 4 m depth) of the water column. The values of all plotted parameters are means and vertical error bar shows \pm 1SD.

plankton communities, which affect carbon cycling and thus modulate microbial activities and oxygen saturation levels of the epilimnetic layer of the reservoir (Figures 3, 4, 5). Interestingly, the more pronounced effects on epilimnetic microbial community dynamics and oxygen saturation levels in the upstream reservoir parts (Figures 4, 5) were related to the actual hydrologic regime rather than to the season. Even though water temperature was clearly higher during interflows and underflows, bacterial abundance, activity, and imbalance toward net heterotrophy was significantly higher during overflows, suggesting that neither water temperature nor water residence

time in the surface layer was playing a principal role in shaping the different patterns found during contrasting hydrological regimes. Although we do not have direct evidence, these results, combined with the strong gradient in BDOC (Table 1) found along the reservoir, strongly support the hypothesis that injection of allochthonous, labile organic carbon enhances epilimnetic microbial activity during overflow events, driving the metabolic balance of the surface layers towards net heterotrophy. Although relative and absolute values of BDOC concentrations sharply dropped towards the lacustrine reservoir parts, in fact the “recalcitrant part” of DOC (that is, the values of

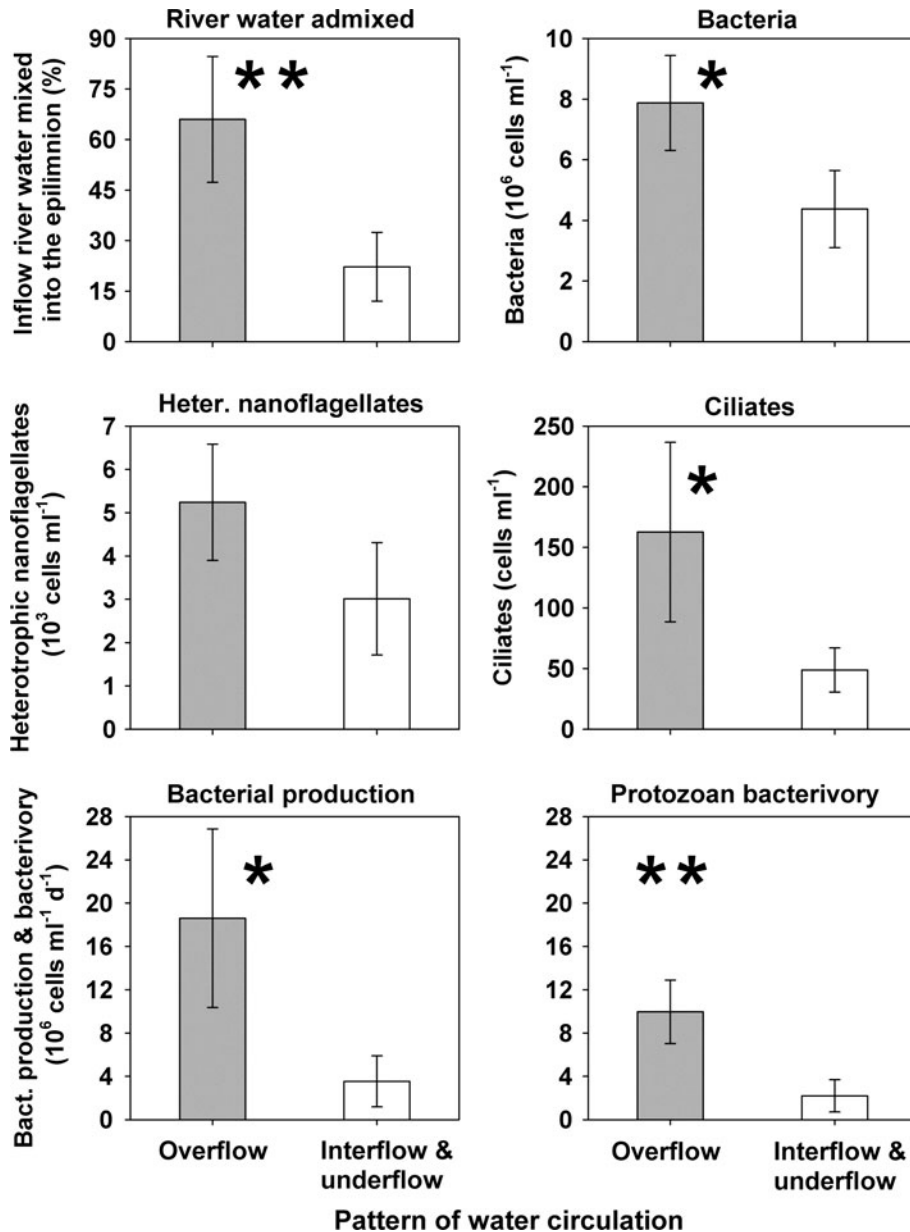


Figure 5. The effect of different water circulation patterns on mean values of microbial parameters from the plunge point and the next three downstream stations plotted separately for overflow (4 sampling campaigns, for details see Table 1) versus pooled inter- and underflow events (4 samplings). The values are means and vertical error bar shows \pm 1SD. Significance differences (*t* test) in means; * $P < 0.05$, ** $P < 0.01$.

DOC minus BDOC concentrations, Table 1) stayed within a very narrow range (2.35–2.50 $mg\ l^{-1}$) throughout the whole longitudinal profile of the reservoir. This again points to the role of labile DOC, which is rapidly processed in the upper inflow parts of the impoundment.

The remarkable effects of hydrology on epilimnetic plankton development were also exemplified by the extremely high abundance of ciliates observed in Feb-98 (205–573 cells ml^{-1} , RDP 0.5–0.8, data not shown), which is an unusual situation for this month (Comerma and others 2003). It likely reflected a flash flood, which induced an overflow current instead of the underflow typical for

winter. Such situations may have important implications in the context of global change in Mediterranean regions, where the expected reductions in runoff (Milly and others 2005) can profoundly affect river water circulation patterns in reservoirs and hence organic carbon cycling in these systems. Our results agree with a recent report relating significant decreases in streamflow to the development of anoxic layers in reservoirs (Marcé and others 2010), and may contribute to establishing the causal link between streamflow and oxygen levels in reservoir ecosystems (Marcé and others 2008). In addition, the results of our study can further promote investigations of such physical predictions in the context

of the role of reservoirs as hot spots for organic carbon processing and CO₂ exchanges with the atmosphere.

Generalizing Trends Induced by Different Water Circulation Patterns

The relative distance model proved to be a useful tool for elucidating and generalizing the spatial trends in abundance and activity of plankton groups suggesting a clear food chain succession from the river to the dam (Figures 3, 4). Interestingly, the overall patterns (Figure 3) were obviously shaped more by the overflow events that strongly influenced oxygen saturation levels and induced the remarkable spatially separated peaks of microbes than inter- and underflow events, which yielded much less pronounced variability downstream from the river inflow (Figures 3, 4, 5). The detailed analyses of specific impacts of overflow events on plankton carbon dynamics affecting oxygen saturation are novel aspects of the study (compare Gasol and others 2002; Comerma and others 2003; Nedoma and others 2006).

We found highly significant relationships between the observed maxima in bacterial abundance, biomass and production and the proportion of nutrient rich river water injected into the reservoir epilimnion, which explained 58–77% of the variability in the bacterial parameters. Thus, the reservoir hydrodynamics regulated the input of dissolved and particulate organic material available to the epilimnetic bacterioplankton and in turn stimulated its dynamics and respiration rates. Notably, the significant negative effects of the overflow events were reflected in sub-saturating oxygen levels ($74 \pm 14\%$, mean \pm SD) in stations within about 5 km downstream of the plunge point compared to the oxygen super saturation ($132 \pm 23\%$) detected when the river water masses plunged below the epilimnion. Our data also suggested that the maxima of bacterivorous protists, that is, HNF and ciliates, were directly proportional to the amount of BDOC-rich river water mixed into the epilimnion (Figure 4). Thus, the later parameter has great potential as a predictor of the development of heterotrophic microbial food webs and accompanying oxygen depletion in the inflow reservoir parts (Figure 4). This may add predictive power to equations predicting carbon processing in reservoir ecosystems, because river water mixing is in fact a physical process included in most customary reservoir dynamical models (Rueda 2006).

Notably, some general features of the processes that induce succession of microbial populations

along the longitudinal axis of this organically loaded reservoir (Table 2; Figures 3, 4, 5) can be compared to a natural “sequential reactor” that reduces the concentration of easily degradable organic material (Uhlmann 1991). The gradual decrease of abundance and activity of bacteria and protozoa and the specific longitudinal changes in oxygen saturation levels (Figure 4) from the plunge point downstream indicated very efficient processes of self-purification. Although selected aspects of these processes have been examined previously (Šimek and others 1998; Armengol and others 1999; Comerma and others 2001), the pooled large data set we analyzed here allowed for broader generalization and deeper insights into the major forces shaping longitudinal succession in this reservoir (Figures 3, 4, 5).

Phytoplankton and zooplankton usually develop downstream at the transitional zone of a reservoir, with peaks often being associated with the plunge point (Kimmel and others 1990). However, the Sau Reservoir displayed quite specific longitudinal patterns of plankton development. For instance, the high nutrient availability (Table 2) should promote massive phytoplankton blooms located much more upstream as observed in other eutrophic reservoirs (Mašín and others 2003). However, the high turbidity of the inflow river water (transparency of only 30–50 cm, Secchi depth), caused by inorganic particles as well as bacteria (Comerma and others 2001; Šimek and others 2001), limits primary production processes at inflow areas (Figures 3, 4). This effect was even more evident for overflow events when the Chl-*a* peaked below the plunge point (Figure 4) where the water is generally more transparent.

High nutrient and organic matter loads (Table 2) resulted in decreased oxygen saturation in the epilimnetic water layers of the riverine and upper transient zones of the reservoir related mainly to the overflow events (Figure 4). This is not at odds with the finding that the oxygen content of the reservoir seems to be mainly controlled by the external load of organic carbon even in the lacustrine part of the reservoir (Marcé and others 2008). Thus, not surprisingly a profound effect of organic carbon loading on oxygen levels was observed near the plunge point and further downstream. Such conditions likely contributed to the unusual longitudinal pattern of zooplankton with almost complete absence of cladocerans and copepods in the riverine zone (Figure 3). Sporadically, only rotifers appeared there in notable abundance. Notably, practically all zooplankton groups had two maxima along the longitudinal axis of the reservoir

at RDP 0.5 and 0.7. However, the first peak of rotifers appeared more upstream (RDP 0.4) and their abundance sharply dropped in the middle reservoir parts, corresponding to the maximum abundance of cladocerans and copepods (Figure 3). Thus competition for food sources or predation on rotifers (Jürgens 1994; Wickham and others 1993) might be responsible for the observed spatial trend.

For reservoir and water quality management it is important to be able to predict how nutrient rich river water flows into and distributes along the length of a reservoir. Although water circulation patterns are mostly temperature controlled, they influence both the development and spatial succession of epilimnetic microbial and phytoplankton communities. Especially for drinking water reservoirs in the Mediterranean area that experience large temporal and even daily fluctuations in river water flow and its quality (Vidal 2007; Marcé and others 2008), such predictions are highly desirable. Our analysis of the impact of overflow circulation events showed strong and statistically significant relationships between the proportion of BDOC-rich river water mixed into the reservoir epilimnion and development of typical heterotrophic microbial food webs. The negative impacts of such events are high inorganic and microbial biomass-related turbidity (for example, Šimek and others 2001) and oxygen depletion even in the epilimnetic layers within extensive upstream parts of the reservoir (Figure 4). Relatively simple data on temperature and other physical and chemical parameters allow for prediction of the type of water circulation. It also can be used as an early warning of the onset of massive heterotrophic processes leading to severe deterioration of water quality for several kilometers downstream of the plunge point of a reservoir. In addition, our approach could also facilitate a comparison of generalized longitudinal succession patterns over a broad variety of reservoir ecosystems. Finally, the tight relationship between hydrological descriptors, organic carbon load, oxygen saturation levels, and bacterial community activity constitutes a first warning on the probable effect of decreasing stream flows on carbon cycling in reservoir ecosystems located in Mediterranean regions.

ACKNOWLEDGMENTS

This study was supported by projects of the Spanish Government (CGL2004-05503-CO2-O1 and CGL2008-06377-CO2-O1), and the Aigues Ter-Llobregat Company. Two of the authors benefited from doctorate grants from the University of Barcelona (M.C. and J.-C. G.). Additional support

was provided by the Grant Agency of the Czech Republic—research grant 206/08/0015, and projects no. AV0Z 60170517. We thank J. Hejzlar for supplying data on proportions of biodegradable organic carbon in total dissolved organic carbon, K. Hornák, J. Jezbera, G. Nurnberg and J. Dolan for their constructive criticisms on earlier manuscript versions and D. Kirchner and K. Edwards for language correction.

REFERENCES

- Armengol J, García JC, Comerma M, Romero M, Dolz J, Roura M, Han BH, Vidal A, Šimek K. 1999. Longitudinal processes in canyon type reservoirs: the case of Sau (N. E. Spain). In: Tundisi JG, Straškraba M, Eds. *Theoretical reservoir ecology and its applications*. Leiden: International Institute of Ecology. Brazilian Academy of Sciences and Backhuys Publishers. p 313–45.
- Bell RT. 1993. Estimating production of heterotrophic bacterioplankton via incorporation of tritiated thymidine. Chapter 56. In: Kemp PF, Sherr BF, Sherr EB, Cole JJ, Eds. *Handbook of methods in aquatic microbial ecology*. London: Lewis Publishers. p 495–503.
- Comerma M, García JC, Armengol J, Romero M, Šimek K. 2001. Planktonic food web structure along the Sau Reservoir (Spain) in Summer 1997. *Internat Rev Hydrobiol* 86:195–209.
- Comerma M, García JC, Armengol J, Romero M, Šimek K. 2003. Carbon flow dynamics in the pelagic community of the Sau Reservoir (Catalonia, NE Spain). *Hydrobiologia* 504:87–98.
- Gasol JM, Comerma M, García JC, Armengol J, Casamayor EO, Kojecká P, Šimek K. 2002. A transplant experiment to identify the factors controlling bacterial abundance, activity, production, and community composition in a eutrophic canyon-shaped reservoir. *Limnol Oceanogr* 47:62–77.
- Grasshoff K, Erhardt M, Kremling K. 1983. *Methods of seawater analysis*. Weinheim: Verlag Chemie.
- Imberger I, Patterson J, Hebbert B, Loh I. 1978. Dynamics of reservoir of medium size. *J Hydraul Div Am Soc Civ Eng* 104:725–43.
- Jeffrey SW, Humphrey GF. 1975. New spectrophotometric equations for determining chlorophylls a, b, c1 and c2 in higher plants, algae and natural phytoplankton. *Biochem Physiol Pflanzen* 167:191–4.
- Jezbera J, Nedoma J, Šimek K. 2003. Longitudinal changes in protistan bacterivory and bacterial production in two differently loaded canyon-shaped reservoirs. *Hydrobiologia* 504:115–30.
- Jürgens K. 1994. Impact of *Daphnia* on planktonic microbial food webs. A review. *Mar Microb Food Webs* 8:295–324.
- Kennedy RH, Walker AW. 1990. Reservoir nutrient dynamics. Chapter 5. In: Thornton KW, Kimmel BL, Payne FE, Eds. *Reservoir limnology: ecological perspective*. New York: Wiley. p 109–31.
- Kimmel BL, Lind OT, Paulson LJ. 1990. Reservoir primary production. Chapter 6. In: Thornton KW, Kimmel BL, Payne FE, Eds. *Reservoir limnology: ecological perspective*. New York: Wiley. p 133–93.
- Marcé R, Comerma M, García JC, Armengol J. 2004. A neuro-fuzzy modelling tool to estimate fluvial nutrient loads in watersheds under time-varying human impact. *Limnol Oceanogr Methods* 2:342–55.

- Marcé R, Moreno-Ostos E, Ordoñez J, Feijoo C, Navarro E, Caputo L, Armengol J. 2006. Nutrient fluxes through boundaries in the hypolimnion of Sau Reservoir: expected patterns and unanticipated processes. *Limnetica* 25:527–40.
- Marcé R, Moreno-Ostos E, Lopes P, Armengol J. 2008. The role of allochthonous inputs of dissolved organic carbon on the hypolimnetic oxygen content of reservoirs. *Ecosystems* 11:1035–53.
- Marcé R, Rodríguez-Arias MA, García JC, Armengol J. 2010. El Niño Southern Oscillation and climate trends impact reservoir water quality. *Global Change Biol* 16:2857–65.
- Mašín M, Šimek K, Jezbera J, Nedoma J, Straškrabová V, Hejzlar J. 2003. Changes in bacterial community composition and microbial activities along the longitudinal axis of two differently loaded canyon-shaped reservoirs. *Hydrobiologia* 504:99–113.
- McCauley E. 1984. The estimation of the abundance and biomass of zooplankton samples. In: Downing JA, Rigler FH, Eds. *Manual on methods for the assessment of secondary productivity in fresh waters*. Oxford: Blackwell Publications. p 228–65.
- Milly PCD, Dunne KA, Vecchia AV. 2005. Global pattern of trends in streamflow and water availability in a changing climate. *Nature* 438:347–50.
- Murphy I, Riley JP. 1962. A modified single-solution method for determination of phosphate in natural waters. *Anal Chim Acta* 27:31–6.
- Nedoma J, García JC, Comerma M, Šimek K, Armengol J. 2006. Extracellular phosphatases in a Mediterranean reservoir: seasonal, spatial, and kinetic heterogeneity. *Freshwat Biol* 51:1264–76.
- Rueda FJ. 2006. Basin scale transport in stratified lakes and reservoirs: towards the knowledge of freshwater ecosystems. *Limnetica* 25:33–56.
- Seda J, Kolářová K, Petrusek A, Macháček J. 2007. *Daphnia galeata* in the deep hypolimnion: spatial differentiation of a “typical epilimnetic” species. *Hydrobiologia* 594:47–57.
- Seitzinger SP, Harrison JA, Dumont E, Beusen AH, Bowman AF. 2005. Sources and delivery of carbon, nitrogen, and phosphorus to the coastal zone: an overview of Global Nutrient Export from Watersheds (NEWS) models and their application. *Global Biogeochem Cycles* 19:GB4S01.
- Servais P, Billen G, Hacoet MC. 1987. Determination of the biodegradable fraction of dissolved organic matter in waters. *Water Res* 21:445–50.
- Šimek K, Bobkova J, Macek M, Nedoma J, Psenner R. 1995. Ciliate grazing on picoplankton in a eutrophic reservoir during the summer phytoplankton maximum: a study at the species and community level. *Limnol Oceanogr* 40:1077–90.
- Šimek K, Armengol J, Comerma M, García JC, Chrzanowski TH, Macek M, Nedoma J, Straškrabová V. 1998. Characteristics of protistan control of bacterial production in three reservoirs of different trophic. *Internat Rev Hydrobiol* 83:485–94.
- Šimek K, Armengol J, Comerma M, García JC, Kojacka P, Nedoma J, Hejzlar J. 2001. Changes in the epilimnetic bacterial community composition, production, and protist-induced mortality along the longitudinal axis of a highly eutrophic reservoir. *Microb Ecol* 42:359–71.
- Solorzano L. 1969. Determination of ammonia in natural waters by the phenol-hypochlorite method. *Limnol Oceanogr* 14:799–801.
- Straškraba M. 1998. Limnological differences between deep valley reservoirs and deep lakes. *Int Review Hydrobiol* 83:1–12.
- Straškraba M, Tundisi JG, Duncan A. 1993. State-of-the-art of reservoir limnology and water quality management. In: Straškraba M, Tundisi JG, Duncan A, Eds. *Comparative reservoir limnology and water quality management*. Dordrecht: Kluwer Academic Publishers. p 213–88.
- Straškrabová V. 1976. Self-purification of impoundments. *Water Res* 9:1171–7.
- Thornton KW, Kimmel BL, Payne FF. 1990. *Reservoir limnology: ecological perspectives*. New York: Wiley. p 246.
- Uhlmann D. 1991. Anthropogenic perturbation of ecological systems: a need for transfer from principles to applications. In: Ravera O, Ed. *Terrestrial and aquatic ecosystems: perturbation and recovery*. Chichester: Ellis Horwood. p 47–61.
- Vidal J. 2007. Basin-scale hydrodynamics in a Mediterranean reservoir. Implications for the phytoplankton dynamics. PhD dissertation, University of Girona, Girona, 166 p.
- Weissenberger S, Lucotte M, Houel S, Soumis N, Duchemin E, Canuel R. 2010. Modeling the carbon dynamics of the La Grande hydroelectric complex in northern Québec. *Ecol Model* 221:610–20.
- Wickham SA, Gilbert JJ, Berninger UG. 1993. Effects of rotifers and ciliates on the growth and survival of *Daphnia*. *J Plankton Res* 15:317–34.